PCCP

Cite this: *Phys. Chem. Chem. Phys.*, 2012, **14**, 11015–11020

www.rsc.org/pccp

PAPER

Excitation energies of retinal chromophores: critical role of the structural model†

Omar Valsson,[a] Celestino Angeli*[b] and Claudia Filippi*[a]

Received 30th April 2012, Accepted 26th June 2012
DOI: 10.1039/c2cp41387f

We employ a variety of highly-correlated approaches including quantum Monte Carlo (QMC) and the *n*-electron valence state perturbation theory (NEVPT2) to compute the vertical excitation energies of retinal protonated Schiff base (RPSB) models in the gas phase. We find that the NEVPT2 excitation energies are in good agreement with the QMC values and confirm our previous findings that the complete-active-space perturbation (CASPT2) approach yields accurate excitations for RPSB models only when the more recent zero-order IPEA Hamiltonian is employed. The excitations computed with the original zero-order formulation of CASPT2 are instead systematically red-shifted by more than 0.3 eV. We then focus on the full 11-*cis* retinal chromophore and show that the M06-2X and MP2 approaches provide reliable ground-state equilibrium structures for this system while the complete-active-space self-consistent field (CASSCF) geometry is characterized by significantly higher ground-state energies at the NEVPT2 and CASPT2 level. Our calibration of the structural model together with the general agreement of all highly-correlated excited-state methods allows us to reliably assign a value of about 2.3 eV to the vertical excitation of 11-*cis* RPSB in the gas-phase.

1 Introduction

The retinal protonated Schiff base (RPSB) chromophore is the light-sensitive molecule present in vertebrate visual opsin proteins, where the interaction with the protein tunes its absorption over a great range of wavelengths from 425 to 560 nm.[1] To understand the spectral properties of this chromophore and distinguish between its intrinsic chemical features and the role of the interaction with the protein environment, the RPSB chromophore has been the subject of extensive theoretical and experimental studies in the gas phase, solution, and protein over the last two decades.[1–39] Many theoretical investigations have focused on the determination of the location of the vertical excitation in the gas phase[20–23,26–28] and, more recently, photo-dissociation experiments have probed the chromophore in the gas phase to assess its absorption properties.[17–19]

The theoretical determination of the vertical excitation of RPSB is complicated by the fact that the the estimate depends rather strongly on the methodology employed both to compute the excitation energy and the equilibrium ground-state geometry. Regarded as a gold standard for the computation of excitation energies,[40] multi-reference perturbation theory (CASPT2) based on complete-active-space self-consistent field (CASSCF) wave functions has often been used in retinal studies in combination with CASSCF ground-state equilibrium geometries.[19,20,31,34,41–45] The two most common choices of zero-order Hamiltonian in CASPT2[46,47] have however been recently shown to produce excitation energies of RPSB systems differing by more than 0.3 eV for the same structural model.[48] Our quantum Monte Carlo (QMC) calculations[48] suggest that the more recent zero-order Hamiltonian, developed to overcome various limitations of the original approach,[47] yields superior results, and that the use of the CASSCF method to determine ground-state equilibrium geometries is not adequate for RPSB and should be abandoned in favor of other approaches such as density functional theory with the M06-2X functional or the MP2 approach.[48,49] Finally, the situation is not less confusing on the experimental side as photo-dissociation spectroscopy has produced multiple spectra, sometimes differing for the same RPSB system.[18,19] Currently, the relation between photo-dissociation and optical absorption spectra is in fact the subject of active investigation and debate.[49–51]

Here, we revisit the long-debated topic of the vertical excitation energies of RPSB models with the use of the *n*-electron valence state perturbation theory (NEVPT2).[52–55] This modern multi-configuration perturbation approach is also based on CASSCF wave functions but relies on a more advanced zero-order Hamiltonian than CASPT2, where all

[a] *MESA+ Institute for Nanotechnology, University of Twente, P.O. Box 217, 7500 AE Enschede, The Netherlands. E-mail: c.filippi@utwente.nl*
[b] *Dipartimento di Chimica, Università di Ferrara, Via Borsari 46, I–44121 Ferrara, Italy. E-mail: anc@unife.it*

† Electronic supplementary information (ESI) available: Additional results for ground-state and vertical excitation energies; equilibrium ground-state geometries of the 11-*cis* RPSB. See DOI: 10.1039/c2cp41387f

bielectronic interactions are explicitly included for the active electrons. The similarity between NEVPT2 and CASPT2 in the zero-order wave function and their difference in the zero-order Hamiltonian renders their comparison quite interesting to elucidate how various ingredients affect such perturbative calculations. Importantly, these NEVPT2 calculations also provide an independent assessment of our QMC and other highly-correlated calculations of the vertical excitation energies of RPSB models.

The paper is organized as follows. In Section 2, we describe the computational details and, in Section 3, introduce the RPSB models we investigate. We present the results for the vertical excitation energies in Section 4 and for the dependence on the choice of structural model in Section 5. Finally, in Section 6, we discuss our results and conclude.

2 Computational details

We employ here the ANO-L-VDZP basis set[56] with the [3s2p1d] contraction on the C and N atoms, and the [2s1p] contraction on the H atoms. As we have shown in our recent studies,[48,49] this basis set yields excitation energies of the minimal RPSB model converged to better than 0.05 eV within both coupled cluster and multi-reference perturbation theory.[48] For the full 11-*cis* retinal, this basis gives even smaller basis-set errors since the corresponding excitation is only 0.01 eV higher than the values obtained with augmentation or a larger [4s3p1]/[3s1p] contraction (see ESI†).

We perform the complete active space self-consistent field (CASSCF) calculations with the MOLCAS[57] and the ORCA 2.8[58–60] codes. In the ORCA calculations for 11-*cis* retinal, the RIJCOSX approximation[61] for the CASSCF steps and the RI approximation[62] for the integral transformation steps are used. Since a corresponding RI auxiliary basis set is not available for the ANO-L-VDZP basis set, we use the aug-cc-pVTZ auxiliary basis set.[63,64] We have adopted and validated this procedure in our recent work on cyanine dyes.[65]

The *n*-electron valence state perturbation theory[52–55] (NEVPT2) calculations in both the partially contracted (PC) and the strongly contracted (SC) variants are performed using the ORCA 2.8 code and a stand-alone code interfaced to MOLCAS. The orbital energies for the doubly occupied and virtual orbitals appearing in the Dyall Hamiltonian[66] (used for the definition of the zero-order Hamiltonian in NEVPT2) are obtained by the diagonalization of a generalization of the Fock operator[67] (canonical orbital option in ORCA). For the NEVPT2 calculations with the ORCA code, in the construction of the third- and fourth-order density matrices for 11-*cis* retinal, the CASSCF wave function is truncated so that only configurations with a weight larger than a threshold of 10^{-10} are kept. As shown in the ESI†, this value for the threshold yields converged results. In the computation of the NEVPT2 excitation energies, we use the same CASSCF wave functions as in our previous CASPT2 study.[48] Specifically, we employ state-average (SA) CASSCF wave functions with equal weights over the two lowest-energy states (S_0 and S_1). The CAS active space consists of all π electrons in the reference and the same number of active π orbitals (see ESI†).

For the CASPT2 calculations, we use two different zero-order Hamiltonians. One Hamiltonian (0-IPEA) is based on a generalization of the Fock operator for multireference wave functions, which was proposed when the CASPT2 approach was first introduced,[46] and has been used in CASPT2 calculations for almost two decades. The second Hamiltonian, named standard IPEA (S-IPEA), is based on a modification (shifting) of the 0-IPEA zero-order Hamiltonian to correct for a systematic error in the original formulation,[47] and is the standard option in the latest versions of MOLCAS. We indicate when a constant imaginary shift[68] is used in the CASPT2 calculations to eliminate intruder-state problems.

The CC3 calculations are performed with the Dalton 2.0 program.[69] The CASPT2, QMC, CC2, and CCSD results are from our previous work,[48] to which we refer the reader for further details. For the DFT geometrical optimizations with the M06-L,[70] M06,[71] M06-2X,[71] and M06-HF[72] functionals and the cc-pVDZ basis set, we use the Gaussian 09 code.[73]

3 Retinal models

The models of RPSB considered in this work are depicted in Fig. 1. They range from the minimal model (A) to the full 11-*cis* chromophore (E). For models A to D, we use the naming convention PSB*x*(*y*) where *x* and *y* indicate the number of double bonds and methyl groups, respectively. For the 11-*cis* chromophore (E), we consider the 6s-*cis*(−) orientation of the β-ionone ring,[49] so the C_5–C_6–C_7–C_8 dihedral angle of the ring with respect to the conjugated chain (denoted ϕ) ranges between −30° and −70° in the various ground-state equilibrium geometries considered here. Unless otherwise stated, the ground-state equilibrium geometries are taken from our previous study[48] and are optimized within DFT with the B3LYP functional and the cc-pVDZ basis set.

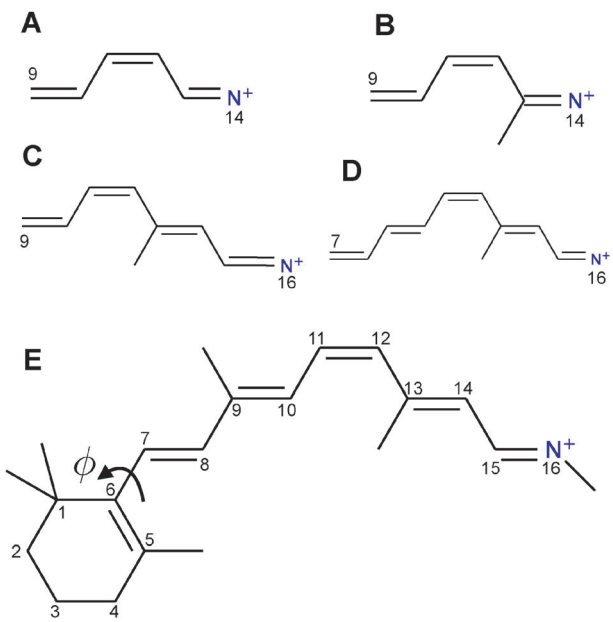

Fig. 1 Model RPSB chromophores: (A) PSB3(0), (B) PSB3(1), (C) PSB4(1), (D) PSB5(1), (E) 11-*cis* chromophore. The naming PSB*x*(*y*) denotes the number of double bonds and methyl groups, *x* and *y*, respectively. The atom numbering for chromophore E is used for all models, so the *cis* bond is always between C_{11} and C_{12}.

4 Vertical excitation energies

In Table 1, we report the vertical excitation energies computed with NEVPT2 and CC3 and the ANO-L-VDZP basis, together with the CC2, CCSD, CASPT2, and DMC results we have previously obtained with the same basis set and geometries.[48] We only list the single-state NEVPT2 and CASPT2 excitation energies since the difference between the corresponding quasi-degenerate NEVPT2 and the multi-state CASPT2 values is negligible for models A, B, and C, and less than 0.06 eV for model D (see ESI†).

For all retinal models, it is immediately evident that the CASPT2 approach with the old 0-IPEA Hamiltonian is at variance with all other highly-correlated methods. The CASPT2/0-IPEA excitation energies are systematically red-shifted by more than 0.3 eV with respect to the values obtained with the other approaches. The use of the standard IPEA Hamiltonian (S-IPEA) significantly improves the CASPT2 results and brings them closer to the NEVPT2, CC, and DMC excitation energies. These findings confirm the superiority of the S-IPEA with respect to the 0-IPEA CASPT2 variant, and the presence of a systematic error in the 0-IPEA approach, which had in fact prompted the CASPT2 developers to propose an improved zero-order Hamiltonian.

Focusing on the multi-reference perturbative approaches, we observe that the NEVPT2 and CASPT2/S-IPEA results are in very good agreement with each other for all retinal models, and within a narrow range of about 0.1 eV. The NEVPT2/PC is the higher quality variant of NEVPT2 and gives the best agreement with CASPT2/S-IPEA. However, both the SC and PC variants of NEVPT2 yield rather similar excitation energies, which is an indication of the good quality of the zero-order wave functions and the consequent reliability of the results.[55,74] Finally, for all retinal models, the difference between the CASSCF excitation energies and the values obtained using the CASPT2/S-IPEA and NEVPT2 methods is rather small and of the order of 10%. This is also a clear indication of a balanced description of the ground and excited states at zero-order, and shows that the effect of the dynamical correlation on the excitation energies is minor in these systems (with the possible exception of the B model). For all these reasons, the CASPT2/S-IPEA and NEVPT2 results can be considered reliable.

Table 1 Vertical excitation energies (eV) of the RPSB models. The results are obtained employing the ANO-L-VDZP basis set and the ground-state DFT/B3LYP equilibrium geometries

Method	A PSB3(0)	B PSB3(1)	C PSB4(1)	D PSB5(1)	E 11-*cis*
SA-CASSCF	4.56	4.80	3.74	3.10	2.51
CASPT2/0-IPEA	3.74	3.85	2.99	2.50	1.85[a]
CASPT2/S-IPEA	4.05	4.17	3.32	2.82	2.20
NEVPT2/PC	4.10	4.22	3.37	2.87	
NEVPT2/SC	4.17	4.28	3.43	2.92	2.26
CC2	4.12	4.20	3.33	2.82	
CCSD	4.23	4.37	3.47	2.95	
CC3	4.11	4.24			
DMC	4.20(2)	4.42(2)	3.47(2)	3.00(3)	2.37(3)

[a] Constant imaginary level shift of 0.1 au.

All other highly-correlated approaches are in good agreement with NEVPT2. In particular, CC2, CC3, and CCSD yield rather similar excitations, with the CC2 values being always red-shifted by about 0.1 eV with respect to CCSD, and very close to CC3 for models A and B. For the 11-*cis* RPSB model, we cannot compute the CC2 excitation energy with the codes we have available but we can compare to the CC2 results of ref. 27, where an excitation energy of 2.10 eV on a B3LYP geometry is reported. The difference between this CC2 value and the corresponding CASPT2 and NEVPT2 excitation energies is therefore larger than for the smaller models, indicating that CC2 might respond differently to the addition of the β-ionone ring.

Finally, the excitations computed within diffusion Monte Carlo are slightly blue-shifted with respect to the NEVPT2 results and in good agreement with CCSD. The only exception is perhaps the B model, where the discrepancy between CCSD and DMC on the one side and the multi-reference perturbative approaches on the other is larger than 0.1–0.2 eV. It should be noted that, for model B, the difference between the CASSCF and PT2 excitations is also larger than for all other models (0.6 eV *versus* 0.3–0.4 eV), indicating a more important role of dynamical correlation. For the 11-*cis* RPSB model, we have here improved the quality of the QMC wave functions with respect to our previous work.[48] In particular, we have further increased the number of configuration state functions (CSF) included in the determinantal component of our Jastrow–Slater wave functions from 10 to 45, by decreasing the threshold imposed on the CSF coefficients from 0.08 to 0.04. The resulting DMC excitation energy is 2.37(3) eV, slightly lower but still compatible with the previous value of 2.41(3) eV.

5 Choice of ground-state geometry

We now focus on the full 11-*cis* chromophore and on how the choice of the structural model affects its vertical excitation energy. In Table 2, we list the CASPT2, NEVPT2, and DMC excitation energies computed on the ground-state geometries optimized within MP2, CASSCF, and DFT with the BLYP, B3LYP, and M06-2X functionals. We also list the ground-state CASPT2/S-IPEA and NEVPT2 energies together with the most important geometrical parameters,[30,49] namely, the bond length alternation (BLA) along the conjugated chain and the angle ϕ of the β-ionone ring. The BLA is here defined as the difference between the averages of the single and double carbon–carbon bond lengths, and computed including the bonds between C_5 and C_{15}.

To optimize the ground-state geometry within DFT, we employ three functionals with a different amount of exact exchange, namely, BLYP (0%), B3LYP (20%), and M06-2X (54%). This choice of DFT functionals is appropriate for retinal as they span a reasonable range of percentage of exact exchange, one of the parameters in the functional which mainly impacts the geometrical features of this system.[30,49] We have recently demonstrated that M06-2X gives a very accurate description of the all-*trans* RPSB chromophore[49] while larger or smaller amounts of exact exchange lead to structures of inferior quality. As shown in Table 2, a similar performance is observed for the 11-*cis* conformer of RPSB

Table 2 Ground-state and vertical excitation energies of the 11-*cis* (E) model computed on the DFT, MP2, and CASSCF ground-state equilibrium geometries. For the BLYP, B3LYP, and M06-2X DFT functionals, the percent of exact exchange is reported in parentheses. The bond length alternation (BLA) and the angle of the β-ionone ring (ϕ, see Fig. 1) are also listed

	Geometry				
	BLYP (0%)	B3LYP (20%)	M06-2X (54%)	MP2	CASSCF[a]
BLA (Å)	0.024	0.033	0.051	0.044	0.101
ϕ (°)	−29.7	−33.5	−38.0	−40.5	−68.8
Ground-state energies (kcal mol^{-1})					
CASPT2/S-IPEA	+3.60	+0.69	0.00	−0.40	+7.01
NEVPT2/SC	+3.99	+0.44	0.00	+0.60	+9.05
Vertical excitation energies (eV)					
SA-CASSCF	2.36	2.51	2.71	2.64	3.25
CASPT2/0-IPEA	1.77[b]	1.85[b]	1.94[b]	1.89[b]	2.27
CASPT2/S-IPEA	2.12	2.20	2.30	2.24	2.61
NEVPT2/SC	2.18	2.26	2.33	2.27	2.60
DMC	2.22(4)[c]	2.37(3)[c]			

[a] CASSCF(12,12)/6-31G* geometry from ref. 20. [b] Constant imaginary level shift of 0.1 au. [c] The threshold on the CSFs is 0.04.

(also see ESI† for geometries optimized with other DFT functionals such as M06-HF). The ground-state NEVPT2 energy is the lowest on the M06-2X geometry while CASPT2 gives an energy only 0.4 kcal mol^{-1} higher than the corresponding value on the MP2 geometry. Overall, the B3LYP, M06-2X, and MP2 equilibrium geometries are of comparably good quality since the corresponding ground-state energies are within 1 kcal mol^{-1} of each other both at the NEVPT2 and CASPT2 level. The ground-state geometry optimized with BLYP (0%) is instead less optimal.

The CASSCF geometry is significantly different from all other geometries, with bond-length alternation and angle of the β-ionone ring almost double than the values for the M06-2X geometry. These features of the CASSCF structure have a marked effect on the NEVPT2/SC and CASPT2/S-IPEA ground-state energies, which are more than 7 kcal mol^{-1} higher than the corresponding values computed on the M06-2X geometry. This confirms our previous findings[49] on the inadequacy of the CASSCF method to describe the geometries of RPSB systems.

As shown in Fig. 2, the vertical excitation energy of the 11-*cis* model is very sensitive to the choice of ground-state structure and to the variations in bond-length alternation and angle of the β-ionone ring as also previously observed in ref. 23, 26 and 30. In going from the BLYP to the CASSCF structure, both geometrical parameters significantly increase and the corresponding excitation energy grows by as much as 0.4–0.5 eV. All highly-correlated approaches display the same trend as a function of the geometry, with CASPT2/S-IPEA and NEVPT2 consistently agreeing within 0.06 eV. As observed for all retinal models in the previous section, the CASPT2/0-IPEA excitations are always red-shifted by about 0.3 eV.

The M06-2X geometry is characterized by a CASPT2/S-IPEA and a NEVPT2 excitation energy of about 2.3 eV and, together with the B3LYP and MP2 structures, defines a rather narrow range of excitations for the 11-*cis* model between 2.20 eV and 2.36 eV. In striking contrast, the

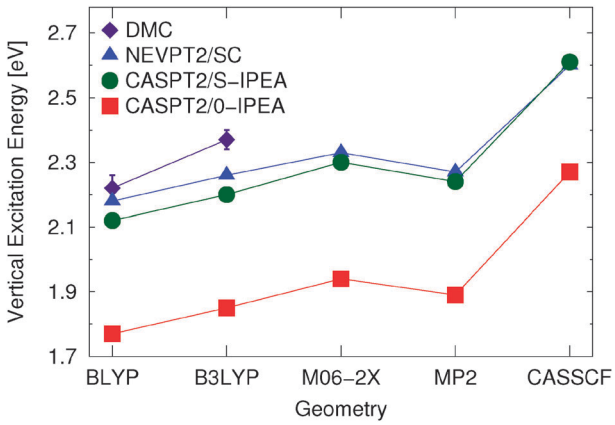

Fig. 2 Vertical excitation energies (eV) of the 11-*cis* retinal (E) model computed on the DFT, MP2, and CASSCF ground-state equilibrium geometries.

CASSCF equilibrium geometry yields excitation energies close to 2.6 eV, that is, more than 0.3 eV blue-shifted with respect to the values at the other geometries. As discussed above, the CASSCF geometry is a less accurate representation of the equilibrium structure of this system and, not surprisingly, is characterized by excitation energies at variance with the ones obtained on more realistic geometries. Finally, it is interesting to note that the CASPT2/0-IPEA excitation energy on the CASSCF geometry is very close to the CASPT2/S-IPEA value at the optimal M06-2X geometry. In the past, this coincidental agreement has masked the inadequacy of the use of CASSCF geometries for retinal. More generally, the use of the CASSCF approach for the calculation of ground-state structures is often coupled to the use of the 0-IPEA zero-order Hamiltonian for the calculation of the CASPT2 excitations, which results in a fortuitous cancellation of errors.[48] Nevertheless, we emphasize again that the results obtained here with a variety of highly-correlated methods clearly indicate that the 0-IPEA approach severely underestimates the excitation energies of retinal and should therefore not be used.

Finally, we note that, for the all-*trans* RPSB chromophore characterized by a similar orientation of the β-ionone ring, we have obtained CASPT2/S-IPEA and NEVPT2 excitation energies of 2.31 eV and 2.34 eV, respectively, when using a M06-2X geometry.[49] These values are very close to the corresponding excitation energies of the 11-*cis* RPSB, demonstrating that the difference between the two isomers does not affect the excitation energies.

6 Discussion and conclusions

We have here extended our previous theoretical study of RPSB models[48] to clarify several important issues, which have been the subject of a lingering debate. To this aim, we have employed the NEVPT2 method which is a modern multi-configuration perturbation approach based on CASSCF wave functions. NEVPT2 relies on a more advanced zero-order Hamiltonian than CASPT2 (all bielectronic interactions among the active electrons are explicitly taken into account), which makes NEVPT2 free from some of the problems affecting CASPT2 as the possible appearance of intruder states.[55] Although based on

different zero-order Hamiltonians, NEVPT2 and CASPT2 share the same methodological framework so that NEVPT2 can serve as an interesting and yet independent test of the results previously obtained by our group[48,49] and other authors.[20–23,26,28] For example, it can help us to understand which zero-order Hamiltonian, S-IPEA or 0-IPEA, should be used in the CASPT2 calculations and further validate the findings obtained with other highly-correlated approaches such as CC or QMC.

For all retinal models, we find that NEVPT2 yields excitation energies rather close to the values computed using the CASPT2/S-IPEA, CC, and DMC methods. The CASPT2/0-IPEA excitation energies are instead systematically red-shifted by more than 0.3 eV with respect to all other results. The overall agreement of the NEVPT2, DMC, and CC methods gives us confidence on the quality of our estimates for the excitation energies of retinal models. Furthermore, our findings support the conclusion that the use of the S-IPEA zero-order Hamiltonian in CASPT2 is superior to the older 0-IPEA variant, which has been so often employed in retinal studies over many years.[19,20,31,34,41–45]

To assess the impact of the choice of ground-state equilibrium geometry on the excitation energy, we then focus on the 11-*cis* retinal. We find that the M06-2X and MP2 methods are reliable approaches to compute the equilibrium structure of this system while the use of the CASSCF method yields a structure characterized by much higher ground-state CASPT2/S-IPEA and NEVPT2 total energies. Furthermore, the geometrical parameters of the CASSCF model (*i.e.* BLA and the orientation of the β-ionone ring) are significantly different from those of the accurate M06-2X geometry. Importantly, these features of the CASSCF geometry strongly affect the excitation energy, which is blue-shifted by as much as 0.3 eV with respect to what is obtained on the better M06-2X structure. The use of CASSCF geometries for retinal systems is quite widespread in studies on the retinal molecule[19,20,31,34,41–45] and has been generally combined with the CASPT2/0-IPEA method for the calculation of the excitation energies. This combination leads to an incorrect description of the system, which is however masked by a fortuitous cancellation of errors in the estimate of the vertical excitation energy (the blue shift due to the use of a CASSCF equilibrium geometry is mostly compensated by an erroneous red shift of the older 0-IPEA variant of CASPT2).

Finally, our calculations with a variety of highly-correlated approaches on reliable ground-state equilibrium geometries define a range of 2.20–2.37 eV for the vertical excitation energy of the 11-*cis* model, with NEVPT2 theory yielding a value of about 2.3 eV on the optimal M06-2X structure. This estimate should be preferably confirmed by experimental findings but a comparison with available experiments is unfortunately problematic. Even though the retinal chromophore has been extensively studied in absorption experiments in solution,[2,9,14] it is difficult to infer an estimate of the gas-phase vertical excitation from these experiments. The absorption spectrum in solution is highly dependent on the particular solvent, and counter-ions induce significant blue shifts in the absorption spectrum since they strongly influence the extended π-electron system of retinal. For instance, the absorption maximum of all-*trans* RPSB in 20 different solvents[2] in the presence of $CHCl_2CO_2^-$ counter-ions ranges between 2.64 and 2.93 eV, and is therefore significantly higher than the expected vertical excitation in the gas phase. Gas-phase photo-dissociation experiments should instead allow a direct comparison with our and other theoretical calculations. However, such comparison is also not straightforward since the relation between photo-dissociation and optical absorption spectra is not simple and is in fact the subject of active investigation and debate.[49–51] For RPSB, early gas-phase photo-dissociation experiments on the 11-*cis* chromophore[18] produced a spectrum with a strong band at 2.03 eV and a broad shoulder of slightly lower intensity, which extends up to 2.34 eV. However, if we consider the experimental evidence on the all-*trans* retinal, which we find to have the same excitation energy as the 11-*cis* conformer, there are two rather different photo-dissociation spectra produced by the same group, one with a main band at 2.00 eV and at least two additional shoulders,[18] and the other with a practically flat plateau between 2.03 eV and 2.34 eV.[19] Here, we will not discuss the interpretation and potential complications of photo-dissociation experiments but only stress that the convergence of our highly-correlated CASPT2, NEVPT2, and DMC excited-state calculations together with our careful calibration of the equilibrium geometry gives us confidence in assigning the vertical excitation of the 11-*cis* RPSB at about 2.3 eV.

Acknowledgements

O.V. and C.F. acknowledge the support from the Stichting Nationale Computerfaciliteiten (NCF-NWO) for the use of the SARA supercomputer facilities. C.A. has been financed by the Italian MIUR through its PRIN 2009 funds.

References

1 T. Ebrey and Y. Koutalos, *Prog. Retinal Eye Res.*, 2001, **20**, 49–94.
2 H. Houjou, Y. Inoue and M. Sakurai, *J. Am. Chem. Soc.*, 1998, **120**, 4459–4470.
3 G. G. Kochendoerfer, S. W. Lin, T. P. Sakmar and R. A. Mathies, *Trends Biochem. Sci.*, 1999, **24**, 300–305.
4 J. Nathans, *Neuron*, 1999, **24**, 299–312.
5 S. Yokoyama, *Prog. Retinal Eye Res.*, 2000, **19**, 385–419.
6 S. T. Menon, M. Han and T. P. Sakmar, *Physiol. Rev.*, 2001, **81**, 1659–1688.
7 R. Stenkamp, S. Filipek, C. Driessen, D. Teller and K. Palczewski, *Biochim. Biophys. Acta*, 2002, **1565**, 168–182.
8 R. E. Stenkamp, D. C. Teller and K. Palczewski, *Arch. Pharm. Pharm. Med. Chem.*, 2005, **338**, 209–216.
9 G. Zgrablić, K. Voïtchovsky, M. Kindermann, S. Haacke and M. Chergui, *Biophys. J.*, 2005, **88**, 2779–2788.
10 K. Palczewski, *Annu. Rev. Biochem.*, 2006, **75**, 743–767.
11 B. Nickle and P. R. Robinson, *Cell Mol. Life Sci.*, 2007, **64**, 2917–2932.
12 J. K. Bowmaker, *Vision Res.*, 2008, **48**, 2022–2041.
13 M. B. Nielsen, *Chem. Soc. Rev.*, 2009, **38**, 913–924.
14 G. Zgrablić, S. Haacke and M. Chergui, *J. Phys. Chem. B*, 2009, **113**, 4384–4393.
15 K. Tsutsui and Y. Shichida, *Photochem. Photobiol. Sci.*, 2010, **9**, 1426–1434.
16 S. O. Smith, *Annu. Rev. Biophys.*, 2010, **39**, 309–328.
17 L. H. Andersen, I. B. Nielsen, M. B. Kristensen, M. O. A. El Ghazaly, S. Haacke, M. B. Nielsen and M. Å. Petersen, *J. Am. Chem. Soc.*, 2005, **127**, 12347–12350.
18 I. B. Nielsen, L. Lammich and L. H. Andersen, *Phys. Rev. Lett.*, 2006, **96**, 018304.
19 J. Rajput, D. Rahbek, L. Andersen, A. Hirshfeld, M. Sheves, P. Altoè, G. Orlandi and M. Garavelli, *Angew. Chem., Int. Ed.*, 2010, **49**, 1790–1793.

20 A. Cembran, R. Gonzalez-Luque, P. Altoe, M. Merchan, F. Bernardi, M. Olivucci and M. Garavelli, *J. Phys. Chem. A*, 2005, **109**, 6597–6605.
21 S. Sekharan, O. Weingart and V. Buss, *Biophys. J.*, 2006, **91**, L07–L09.
22 K. Bravaya, A. Bochenkova, A. Granovsky and A. Nemukhin, *J. Am. Chem. Soc.*, 2007, **129**, 13035–13042.
23 R. Send and D. Sundholm, *Phys. Chem. Chem. Phys.*, 2007, **9**, 2862–2867.
24 R. Send and D. Sundholm, *J. Phys. Chem. A*, 2007, **111**, 27–33.
25 R. Send and D. Sundholm, *J. Phys. Chem. A*, 2007, **111**, 8766–8773.
26 A. Altun, S. Yokoyama and K. Morokuma, *J. Phys. Chem. B*, 2008, **112**, 16883–16890.
27 R. R. Zaari and S. Y. Wong, *Chem. Phys. Lett.*, 2009, **469**, 224–228.
28 R. Send, V. R. I. Kaila and D. Sundholm, *J. Chem. Theory Comput.*, 2011, **7**, 2473–2484.
29 U. F. Röhrig, L. Guidoni and U. Rothlisberger, *ChemPhysChem*, 2005, **6**, 1836–1847.
30 M. Wanko, M. Hoffmann, P. Strodel, A. Koslowski, W. Thiel, F. Neese, T. Frauenheim and M. Elstner, *J. Phys. Chem. B*, 2005, **109**, 3606–3615.
31 P. B. Coto, A. Strambi, N. Ferré and M. Olivucci, *Proc. Natl. Acad. Sci. U. S. A.*, 2006, **103**, 17154–17159.
32 M. Hoffmann, M. Wanko, P. Strodel, P. H. König, T. Frauenheim, K. Schulten, W. Thiel, E. Tajkhorshid and M. Elstner, *J. Am. Chem. Soc.*, 2006, **128**, 10808–10818.
33 K. Fujimoto, J.-Y. Hasegawa and H. Nakatsuji, *Chem. Phys. Lett.*, 2008, **462**, 318–320.
34 G. Tomasello, G. Olaso-González, P. Altoeà, M. Stenta, L. Serrano-Andreás, M. Merchaán, G. Orlandi, A. Bottoni and M. Garavelli, *J. Am. Chem. Soc.*, 2009, **131**, 5172–5186.
35 H. C. Watanabe, Y. Mori, T. Tada, S. Yokoyama and T. Yamato, *Biophysics*, 2010, **6**, 67–78.
36 R. Rajamani, Y.-L. Lin and J. Gao, *J. Comput. Chem.*, 2011, **32**, 854–865.
37 S. Sekharan and K. Morokuma, *J. Am. Chem. Soc.*, 2011, **133**, 19052–19055.
38 J. S. Frähmcke, M. Wanko and M. Elstner, *J. Phys. Chem. B*, 2012, **116**, 3313–3321.
39 V. R. I. Kaila, R. Send and D. Sundholm, *J. Phys. Chem. B*, 2012, **116**, 2249–2258.
40 D. Roca-Sanjuán, F. Aquilante and R. Lindh, *WIREs Comput. Mol. Sci.*, 2012, **2**, 585–603.
41 M. Garavelli, P. Celani, F. Bernardi, M. A. Robb and M. Olivucci, *J. Am. Chem. Soc.*, 1997, **119**, 6891–6901.
42 R. González-Luque, M. Garavelli, F. Bernardi, M. Merchán, M. A. Robb and M. Olivucci, *Proc. Natl. Acad. Sci. U. S. A.*, 2000, **97**, 9379–9384.
43 T. Andruniów, N. Ferré and M. Olivucci, *Proc. Natl. Acad. Sci. U. S. A.*, 2004, **101**, 17908–17913.
44 A. Cembran, R. González-Luque, L. Serrano-Andrés, M. Merchán and M. Garavelli, *Theor. Chem. Acc.*, 2007, **118**, 173–183.
45 I. Schapiro, M. N. Ryazantsev, L. M. Frutos, N. Ferré, R. Lindh and M. Olivucci, *J. Am. Chem. Soc.*, 2011, **133**, 3354–3364.
46 K. Andersson, P.-A. Malmqvist, B. O. Roos, A. J. Sadlej and K. Wolinski, *J. Phys. Chem.*, 1990, **94**, 5483–5488.
47 G. Ghigo, B. O. Roos and P.-Å. Malmqvist, *Chem. Phys. Lett.*, 2004, **396**, 142–149.
48 O. Valsson and C. Filippi, *J. Chem. Theory Comput.*, 2010, **6**, 1275–1292.
49 O. Valsson and C. Filippi, *J. Phys. Chem. Lett.*, 2012, **3**, 908–912.
50 K. Chingin, R. M. Balabin, V. Frankevich, K. Barylyuk, R. Nieckarz, P. Sagulenko and R. Zenobi, *Int. J. Mass Spectrom.*, 2011, **306**, 241–245.
51 M. W. Forbes, A. M. Nagy and R. A. Jockusch, *Int. J. Mass Spectrom.*, 2011, **308**, 155–166.
52 C. Angeli, R. Cimiraglia, S. Evangelisti, T. Leininger and J.-P. Malrieu, *J. Chem. Phys.*, 2001, **114**, 10252–10264.
53 C. Angeli, R. Cimiraglia and J.-P. Malrieu, *Chem. Phys. Lett.*, 2001, **350**, 297–305.
54 C. Angeli, R. Cimiraglia and J.-P. Malrieu, *J. Chem. Phys.*, 2002, **117**, 9138–9153.
55 C. Angeli, M. Pastore and R. Cimiraglia, *Theor. Chem. Acc.*, 2007, **117**, 743–754.
56 P. Widmark, P. Malmqvist and B. O. Roos, *Theor. Chem. Acc.*, 1990, **77**, 291–306.
57 F. Aquilante, L. De Vico, N. Ferré, G. Ghigo, P.-A. Malmqvist, P. Neogrády, T. B. Pedersen, M. Pitoňák, M. Reiher, B. O. Roos, L. Serrano-Andrés, M. Urban, V. Veryazov and R. Lindh, *J. Comput. Chem.*, 2010, **31**, 224–247.
58 F. Neese, *ORCA – an ab initio*, Density Functional and Semiempirical program package, Version 2.8., Max-Planck-Insitut für Bioanorganische Chemie, Mülheim an der Ruhr, 2011.
59 F. Neese, *WIREs Comput. Mol. Sci.*, 2012, **2**, 73–78.
60 F. Neese, D. G. Liakos and S. Ye, *JBIC, J. Biol. Inorg. Chem.*, 2011, **16**, 821–829.
61 F. Neese, F. Wennmohs, A. Hansen and U. Becker, *Chem. Phys.*, 2009, **356**, 98–109.
62 K. Eichkorn, O. Treutler, H. Öhm, M. Häser and R. Ahlrichs, *Chem. Phys. Lett.*, 1995, **240**, 283–289.
63 T. H. Dunning Jr, *J. Chem. Phys.*, 1989, **90**, 1007–1023.
64 F. Weigend, A. Köhn and C. Hättig, *J. Chem. Phys.*, 2002, **116**, 3175.
65 R. Send, O. Valsson and C. Filippi, *J. Chem. Theory Comput.*, 2011, **7**, 444–455.
66 K. G. Dyall, *J. Chem. Phys.*, 1995, **102**, 4909–4918.
67 C. Angeli, R. Cimiraglia and J.-P. Malrieu, *Chem. Phys. Lett.*, 2000, **317**, 472–480.
68 N. Forsberg and P.-Å. Malmqvist, *Chem. Phys. Lett.*, 1997, **274**, 196–204.
69 DALTON, an *ab initio* electronic structure program, release 2.0, see http://www.kjemi.uio.no/software/dalton/dalton.html, 2005.
70 Y. Zhao and D. G. Truhlar, *J. Chem. Phys.*, 2006, **125**, 194101.
71 Y. Zhao and D. G. Truhlar, *Theor. Chem. Acc.*, 2008, **120**, 215–241.
72 Y. Zhao and D. G. Truhlar, *J. Phys. Chem. A*, 2006, **110**, 13126–13130.
73 M. J. Frisch, G. W. Trucks, H. B. Schlegel, G. E. Scuseria, M. A. Robb, J. R. Cheeseman, G. Scalmani, V. Barone, B. Mennucci, G. A. Petersson, H. Nakatsuji, M. Caricato, X. Li, H. P. Hratchian, A. F. Izmaylov, J. Bloino, G. Zheng, J. L. Sonnenberg, M. Hada, M. Ehara, K. Toyota, R. Fukuda, J. Hasegawa, M. Ishida, T. Nakajima, Y. Honda, O. Kitao, H. Nakai, T. Vreven, J. A. Montgomery, Jr., J. E. Peralta, F. Ogliaro, M. Bearpark, J. J. Heyd, E. Brothers, K. N. Kudin, V. N. Staroverov, R. Kobayashi, J. Normand, K. Raghavachari, A. Rendell, J. C. Burant, S. S. Iyengar, J. Tomasi, M. Cossi, N. Rega, J. M. Millam, M. Klene, J. E. Knox, J. B. Cross, V. Bakken, C. Adamo, J. Jaramillo, R. Gomperts, R. E. Stratmann, O. Yazyev, A. J. Austin, R. Cammi, C. Pomelli, J. W. Ochterski, R. L. Martin, K. Morokuma, V. G. Zakrzewski, G. A. Voth, P. Salvador, J. J. Dannenberg, S. Dapprich, A. D. Daniels, Ö. Farkas, J. B. Foresman, J. V. Ortiz, J. Cioslowski and D. J. Fox, *Gaussian 09 Revision A.02*, Gaussian Inc., Wallingford CT, 2009.
74 C. Angeli and M. Pastore, *J. Chem. Phys.*, 2011, **134**, 184302.

